Experimentally Observed Features of the Turbulent Near-Wake of a Model Ship

Vincent G. Johnston and David T. Walker
Department of Naval Architecture & Marine Engineering

Contract Number N000184-86-K-0684
Technical Report No. 92-1

January 1992

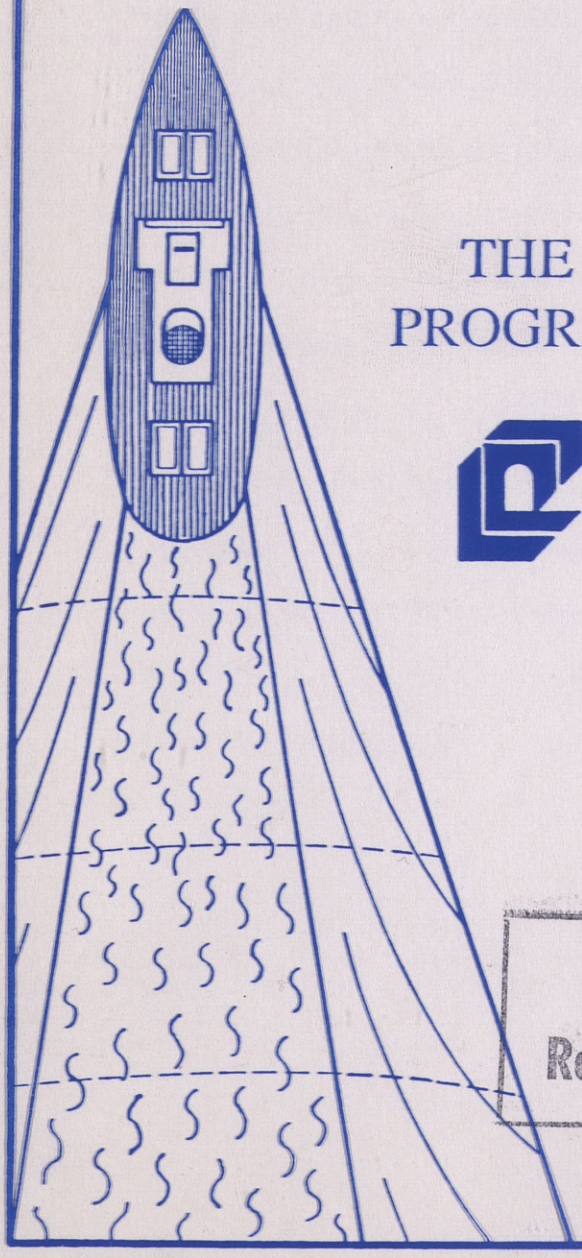

THE UNIVERSITY OF MICHIGAN
PROGRAM IN SHIP HYDRODYNAMICS

COLLEGE OF ENGINEERING

NAVAL ARCHITECTURE &
MARINE ENGINEERING

AEROSPACE ENGINEERING

MECHANICAL ENGINEERING &
APPLIED MECHANICS

SHIP HYDRODYNAMIC
LABORATORY

SPACE PHYSICS RESEARCH
LABORATORY

ERIM

THE UNIVERSITY OF MICHIGAN
PROGRAM IN SHIP HYDRODYNAMICS

COLLEGE OF ENGINEERING

NAVAL ARCHITECTURE &
MARINE ENGINEERING

AEROSPACE ENGINEERING

MECHANICAL ENGINEERING &
APPLIED MECHANICS

SHIP HYDRODYNAMIC
LABORATORY

SPACE PHYSICS RESEARCH
LABORATORY

ERIM

Experimentally Observed Features of the Turbulent Near-Wake of a Model Ship

Vincent G. Johnston and David T. Walker
Department of Naval Architecture & Marine Engineering

Contract Number N000184-86-K-0684
Technical Report No. 92-1

January 1992

Submitted to: Journal of Ship Research
December 1991

Experimentally Observed Features of the Turbulent Near-Wake of a Model Ship

Vincent G. Johnston and David T. Walker

Department of Naval Architecture and Marine Engineering
The University of Michigan, Ann Arbor, MI 48109-2145.

Flow visualization techniques are used to study the turbulent wake of a model ship, with and without propulsion, for distances up to two ship-lengths aft. The turbulent wake is characterized by a thin, rapidly spreading, surface-current layer and a central vertical region of turbulent fluid, resulting in a "tee" shape for the near wake. The turbulent surface layer spreads more rapidly in the propelled case than in the non-propelled case. The only large-scale coherent vortices observed in the subsurface wake were a pair of inboard rotating turbulent vortices produced in the stern cavities on either side of the rudder. These vortices diffuse quickly and do not appear to affect the free surface. For distances less than two ship lengths aft, there is a region of unsteady, irregular free-surface disturbances which corresponds to the subsurface region of turbulent flow. At the edges of this turbulent region, the small scale disturbances created by the turbulence coalesce into relatively organized, but unsteady, waves which are independent of the Kelvin wave pattern. These organized waves propagate outward into the irrotational free stream, and may be related to surface ship wake signatures obtained via synthetic aperture radar techniques.

Introduction

The free-surface aspects of ship hydrodynamics have received increasing attention in recent years. A significant portion of this interest has come as a result of developments in remote sensing which are expected to allow worldwide monitoring of maritime traffic in the foreseeable future. Techniques such as synthetic aperture radar (SAR) are capable of detecting the free-surface disturbances created by a surface ship many kilometers behind the vessel, and sometimes many hours after the ship has passed (Munk *et al.*[1]). The hydrodynamic phenomena associated with the free-surface features of ship wakes include the steady Kelvin wave pattern, breaking waves, and the turbulent wake, as well as the interactions of all of these with wind generated waves, surfactants, etc. Presently, our lack of a clear understanding of some of the dominant physical mechanisms associated with these phenomena has prevented a complete explanation of the SAR signatures of surface ships. This study examined one significant component of the complex collection of hydrodynamic phenomena which comprise a ship wake, the turbulent wake that evolves aft of the ship in the presence of, and interacting with, the free surface. The objectives of this study were to identify qualitative features of both the subsurface turbulent flow and the resulting free-surface disturbances in the near-wake of a model ship, and to determine the relationship between these features.

SAR images of the ocean surface in light wind, or no wind conditions (no small-scale waves) appear dark (no radar return). In moderate to heavy wind conditions, radar images appear gray due to return from the ambient, wind generated waves. When surface ships pass through the ambient wave field, a dark region in the radar image is seen trailing the ship along its path (Lyden *et al.* [2]). This is a region of weak radar return and is made visible by the return from the ambient waves surrounding it. Another feature, a bright

"vee" with an included angle of about three to seven degrees, is seen extending aft of the ship with its apparent vertex located slightly ahead of the ship (Lyden *et al.*). This "vee" encloses the dark centerline feature, although it does not extend nearly as far aft.

Lyden *et al.* [2] proposed that the absence of radar return from the dark centerline region is due to modification of the ambient wave field due to surface currents in the wake. Peltzer *et al.* [3] suggest that collection of surfactant bands at the edge of the wake attenuates waves entering the centerline region.

Milgram [4] and others have suggested that the bright "vee" feature of the SAR return results from Bragg scattering of the electromagnetic field from small, centimeter scale waves. Several explanations have been offered for the generation of these short wavelength waves. Hughes [5] and Munk *et al.* [1] propose that unsteady surface disturbances in the turbulent wake act as random sources that continuously generate small-scale disturbances. It has also been proposed (Milgram [4]) that the Bragg scattering waves consistent with SAR images result from ship generated diverging waves located inside the cusp lines of the Kelvin wake. However, as discussed by Munk *et al.* [1], the Kelvin wave pattern probably can not produce the symmetric signatures observed. Another possible explanation offered by Griffin [6] is that Bragg-wavelength waves are produced through modification of features of the Kelvin wake due to the interaction with the velocity defect in the wake. For reasonable velocity defects, this results in bright "vee" wakes with included angles which are larger than those usually observed. Lyden *et al.* [2] proposed that the bright "vee" is caused by the steepening of ambient waves near the edge of the wake. This steepening is attributed to diverging flow in the wake caused by the presence of counter-rotating "bilge" vortices (see e.g. Lugt [7]).

Experimental investigations of turbulent flows near free surfaces have been limited primarily to turbulent jets issuing beneath, and parallel to, a free surface. Ramberg *et al.* [8] made turbulence measurements in a developing planar surface jet and noted a decrease in vertical velocity fluctuations near the free surface. The interaction of a round turbulent jet issuing parallel to a free surface was examined by Madnia [9] (see also Anthony *et al.* [10] and Bernal & Madnia [11]). Regions of significant surface disturbance were identified and the appearance of small circular dimples on the free surface was noted. These dimples are typical of the signature of a vortex with its axis normal to the free surface (see Sterling *et al.* [12]). The study of Anthony [13] and Anthony *et al.* [9] examined a circular jet issuing two jet diameters below, and parallel to, a free surface using a three component laser velocimeter. They also noted that the vertical velocity fluctuations were damped near the free surface and identified several other interesting effects. Most notable of these was the existence of a thin surface-current layer, identified by near surface velocity measurements, which propagated away from the jet centerline. This behavior was confirmed using flow visualization.

In summary, surface ships can produce distinct synthetic aperture radar signatures and there are many proposed explanations for these. As noted above, there has been little experimental work in the interaction of turbulent flows with a free surface. The purpose of this study is to examine the turbulent wake of a model ship in order to determine the overall qualitative behavior of the wake. In addition, some of the details of the interaction between the subsurface turbulence and the free surface are investigated in an attempt to identify features which may be related to the distinct SAR signatures created by ship wakes. The turbulent wake is investigated using fluorescent dye visualization of the subsurface wake and shadowgraph visualization of the free-surface features. Results presented will show

that the wake is characterized by a thin, rapidly growing surface-current layer resulting in a "tee" shape when viewed in cross-section. Furthermore, no large-scale coherent vortices which directly affect the free-surface features were observed in the wake. Also, the turbulence near the free surface generates unsteady surface disturbances which coalesce at the edge of the wake and propagate outward as relatively organized waves aligned at a small angle relative to the ship track.

Experimental apparatus and procedures

Experimental apparatus

Flow visualization experiments were carried out using a 1/12 scale model of the 62.5 m long U.S. Navy ocean-going fleet tug *Quapaw*. This ship has been used extensively in full-scale wake remote sensing studies. The model is 4.95 m in length, with a beam of 0.95 m, and a maximum draft of 0.43 m (Figure 1). A turbulence generating sand strip placed 0.2 m aft of the bow was used to insure turbulent flow along the full length of the model. The model was towed in the 6.70 m x 3.05 m cross-section, 109.7 m long model basin in the University of Michigan Ship Hydrodynamics Laboratory. The model was towed using an electrically driven carriage with a speed range of 0.8 to 6.1 m/s. The model was affixed to the carriage by means of a heave staff, which was which is free to move in the vertical direction. Fore and aft stabilizers that restricted yaw and roll motions were also employed.

Tests were run both with and without a right-hand rotating propeller on the model. The four bladed propeller has a 30.5 cm diameter, with a pitch to diameter ratio equal to 1.083, a propeller area to disc area ratio equal to 0.382, and a mean width ratio of 0.24. For the propelled tests, the speed of the propeller was set so that the thrust generated was equal to the drag on the model, as indicated by a force dynamometer attached to the model

tow point. As a result, the momentum flux introduced by the propeller exactly balances the sum of the wave drag and the viscous drag. This is contrary to the normal practice in ship model tests; usually the thrust coefficient is set equal to the drag coefficient for the full-scale ship at equal Froude number. The normal practice results in a smaller momentum excess in the model ship wake than would occur at full scale. This is due to the larger viscous drag caused by operating the model at lower Reynolds number than the full-scale ship. For these tests, it was felt that the momentum balance in the wake should reflect the actual viscous drag on the model and not be altered to account for the lower viscous drag which would occur at full scale. It is recognized, however that this practice will result in more swirl in the thrust wake than would occur at full scale.

Two methods were used to examine the qualitative features of the turbulent near-wake. A fluorescent dye visualization technique was used for examining the evolution of the subsurface turbulent wake, and a shadowgraph technique was used for visualizing free-surface disturbances in the wake. The turbulent wake was examined at model velocities of 1.11, 1.48, and 2.23 m/s in the region up to two ship lengths behind the model, both with and without a propeller on the model. These velocities are equivalent to Froude numbers of 0.16, 0.21, and 0.32 respectively. For the three cases the Reynolds number of the resulting turbulent wake (based on wake width and free-stream velocity) was in excess of 10^5.

Fluorescent dye visualization

The subsurface turbulent wake was visualized by marking the boundary layer fluid with a fluorescent dye and examining the evolution of the marked fluid (the turbulent wake) behind the model. A syringe was used to inject 50 cc of a 1000 p.p.m. Rhodamine B/water solution per experimental run, into the boundary layer through a 1.587 mm inner

diameter, 3.175 mm outer diameter Tygon tube wrapped around the model. For some of the runs, the tube was fixed 1/4 ship length aft of the bow. Four injection points were made by drilling 1.42 mm diameter holes through both sides of the tubing at four locations. In this arrangement, the lower holes were spaced at 0.3 m and 0.6 m from the keel, and the uppermost injection holes were located approximately 100 mm below the free surface when the model was at rest. Several experimental cases were performed with the dye injection tube located at the midship location. Due to the larger circumference of the model at this location, two additional injection holes were placed in the injection tube making six total. Again each of the holes were spaced 0.3 m to either side of the keel. Additional holes were located at 0.3 m increments around the circumference of the model. The uppermost holes were just below the free surface. The additional holes allowed a larger portion of the boundary layer to be marked. This ensured that the phenomena identified were not an artifact of the injection locations chosen. At both of the injection tube locations, the turbulent boundary layer was relatively thick so that there was no observable flow disturbance or boundary layer separation due to the tube. During a run, dye injection was initiated two ship lengths before passing through the laser sheet and concluded after the ship had completely passed through the laser sheet.

The evolution of the dye-marked boundary layer and wake was examined using a two-dimensional sheet of laser light which was stationary in the model basin and oriented normal to the path of the model. The multi-line beam of an argon-ion laser operating at approximately 2 W output power was formed into a sheet using a light-weight, first-surface aluminum mirror attached to a galvanometer that was oscillated at 60 Hz. The galvanometer was located 100 mm below the still water level in a submerged glass housing with the laser sheet directed such that the top of the sheet intersected the free surface at the

lateral midship location (see Figure 2). As the fluorescent dye passed through the laser sheet, the emitted light yielded a cross-sectional view of the dye concentration distribution in the plane of the laser sheet. Due to the arrangement described above, the intensity of the laser sheet decreases in the direction of propagation (right to left in the results presented below); hence, the fluorescent emission from the dye also decreases in this direction. The fluorescent emission from the dye was recorded using a submerged CCD camera in a water tight housing.

Shadowgraph imaging

A shadowgraph technique was used to examine the behavior of the free surface in the moving (ship) reference frame. In this implementation of the technique, a translucent screen was placed a small distance above the water surface and a point source of light was placed far below the surface. Any deformation of the free surface results in refraction of the light at the air-water interface and a corresponding change in the light intensity incident on the screen. Surface deformations which result in convex curvature act in a manner similar to a positive lens and, therefore, concentrate light on the screen. Surface deformations which result in concave curvature act like a negative lens and reduce the intensity of the light on the screen. It follows then, that local surface elevations will result in bright regions on the shadowgraph screen, while surface depressions will result in corresponding dark regions. The distance of the screen above the free surface serves to select the range of surface curvatures to which the technique is sensitive. Surface deformations with curvatures on a scale smaller than the distance between the free surface and the screen are not captured.

The shadowgraph screen was 1.21 m square and was located 50 mm above the free surface. It was placed at four locations aft of the model, 1/4, 1/2, 1, and 2 ship lengths, as

shown in Figure 3. For all these locations, the screen was either centered on the centerline of the turbulent wake or offset from the wake centerline by 0.5 m. The light source for these experiments was a 300 W tungsten flood lamp located 1.7 m below the free surface. Images of the shadowgraph screen were recorded at a framing rate of 30 Hz, but an electronic shutter was employed to yield an exposure time of 1/1000 s for each frame. The camera arrangement is also shown in Figure 3.

Images from both the dye visualization and the shadowgraph experiments were recorded using an optical disk recorder. Individual frames were captured using an 8-bit Data Translation DT2255-60 frame-grabber operating in an Apple Macintosh IIfx. Some dye visualization images were enhanced by adjusting the contrast to make the dye more visible. Shadowgraph images were modified by removing the background light intensity distribution which results from the point-source illumination.

For some of the shadowgraph results presented below, the steady free-surface features were examined by averaging several images at the same conditions, from widely-spaced points in time. These averaged shadowgraph images were calculated by digitizing each video image to obtain a 640 x 480 element, two-dimensional array of 8-bit grayscale values. The resulting arrays were then summed, element by element, and divided by the number of frames.

Results and discussion

Subsurface wake

Figure 4 shows a sequence of images of the subsurface flow for the model operating at a velocity of 1.11 m/s with no propeller. In this sequence, the image locations are given in terms of model ship length L for the variable x, where $x = 0$ corresponds to the model propeller plane and positive x is the distance aft of the propeller plane. The locations range

from $x = -1/2L$ to $x = L$. At the same location as the laser sheet, a submerged 1000 W light illuminates the model so that the body surface streamlines can be seen. The dye injection tube for this case is located at $x = -1/2L$.

Tracing the dye along the model hull in Figures 4a and 4b, shows no apparent flow separation or "bilge" vortices. This was verified by extensive visualization using numerous injection locations. The initial shape of the turbulent portion of the wake, shown in Figure 4d, is characterized by a thin layer of turbulent fluid near the surface with a vertical region centered below resulting in a "tee" shape. The vertical region initially extends to a depth about equal to the draft of the model. The thin, turbulent surface layer is similar to the behavior seen by Anthony [12] in a near-surface turbulent jet. Velocity measurements done by Anthony [12] showed that this turbulent layer near the surface exhibited a strong outward velocity component (away from the centerline).

A more detailed fluorescent dye flow visualization of the model ship boundary layer and initial formation of the wake is shown in Figure 5 for a velocity of 1.48 m/s. The dye injection tube was placed at $x = -3/4L$, or one quarter of a ship length aft of the bow. Only two injection points were placed on each side of the model. These injection locations mark the fluid near the surface, and hence the surface-current layer, and the fluid that moves down near the keel of the model at the midship location. In these figures the video camera was placed half a ship length aft of the laser sheet with a field of view of 1.37 m x 1.02 m for the images. The images in the left and right columns of Figure 5 are for the same x-locations: The left column shows the results with no propeller and the right column shows those for the model with a right-hand rotating propeller.

As the model moves through the laser sheet (forward into the page), the dyed fluid is seen distinctly in the boundary layer and its path can be traced along the hull. The behavior

of the boundary layer fluid is very similar for both the propelled and non-propelled cases up to the point where the fluid passes the propeller plane. Figures 5c through 5f show the initial formation of two inboard rotating vortices as the turbulent boundary layer approaches the propeller plane. These are stern vortices, as described by Lugt [7]. However, a short distance downstream, at $x = 1/4L$ (Figures 5i and 5j), there is little evidence of any distinct, large-scale vortical structure. In this case the turbulence in the boundary layer fluid is sufficient to diffuse the concentrated vorticity associated with the stern vortices. These regions remain highly turbulent with small mean circulation, and in the unpropelled case, eventually interact to carry a portion of the turbulent wake fluid downward, away from the free surface. The behavior of the remnants of the stern vortices is less clear in the propelled case. Interaction with the swirling propeller wake appears to limit the downward movement. Extensive visualization of the turbulent boundary layer and wake showed no other observable large-scale vortical structure.

As in Figure 4, the wake cross-section shown in Figure 5 has the characteristic "tee" shape, with a thin layer of turbulent fluid near the surface and a vertical region centered below. The addition of the propeller adds a swirl component to the wake. This seems to cause the vertical region of dyed fluid to be swept slightly to the port side of the wake centerline. The wake of the propelled model grows more quickly in all directions. This is probably due to the higher turbulence levels present in the propelled wake due to its increased momentum.

Similar results were obtained for model velocities of 1.11 m/s and 2.23 m/s. At the higher velocity, dye visualizations become more difficult because of the reduced concentration of dye at each cross sectional plane, resulting in a loss of contrast in the

images. However, the wake for the higher velocity case appears to grow more quickly than the other cases. This is, again, probably due to higher turbulence levels in the wake.

The dominant characteristics for both the propelled and non-propelled cases appear to be quite similar. This suggests that the model hull, and not the effects of propulsion, may represent the key factor in the development and shape of the subsurface wake, with additional momentum introduced by the propeller serving to accelerate the development process. Further, similarities between these wake results and the turbulent jet visualization of Anthony [12] suggests that the exact geometry of the wake generating form may not be critical.

Free-surface features

Figures 6 through 9 show the free surface in the turbulent wake region, as visualized using the shadowgraph technique. The wake images are oriented such that the forward travel direction of the ship is from the bottom of the image toward the top. The field of view in each of the shadowgraph images is 1.1 m square. In situations where a location aft of the model is given for a shadowgraph image, the location is referenced to the center of the image. In each figure the left hand column images are cases in which there was no propeller attached to the model, and the right hand column images are cases including the rotating propeller, with otherwise identical conditions.

In Figure 6 the screen is centered relative to the wake centerline. The model ship velocity is 1.48 m/s and the images are for locations x = 1/4L, 1/2L, L, and 2L. Apparent in these images are unsteady, small-scale, surface disturbances which are generated by turbulent velocity and pressure fluctuations in the wake and propagate in all directions. Disturbances which are moving outward, away from the wake centerline, appear to coalesce into somewhat organized waves as they leave the turbulent region and propagate

into the irrotational free-stream flow. As the distance aft increases, the magnitude of disturbance to the free surface decreases. By $x = 2L$ (Figures 6g and 6h), the surface is relatively calm. There is a noticeable increase in surface disturbances caused by the rotating propeller, particularly on the starboard side of the wake. The swirl of the propeller also appears to move the turbulent fluid to the starboard side of the wake and creates a region of calm water near the wake centerline. The increase in near-surface turbulence also causes an increase in the amplitude of the organized waves at the edges of the wake. The width of the turbulent region of the wake is also slightly increased by the rotating propeller.

The shadowgraph images of the turbulent region are also populated by numerous small, circular dark spots. These spots are characteristic of signatures generated by vortices with their axes of rotation oriented normal to the free surface (see Sterling *et al.* [12]). These features indicate that vortex reconnection is a prominent feature in the behavior of the turbulent wake. The scale of these signatures is considerably smaller than that of the wake itself. This is in contrast to the jet results of Anthony [12] which showed reconnection occurring at scales near the largest scales present. This may result from the lack of a well defined large-scale vortical structure in the near-wake. Since the wake is made up of fluid from the boundary layers, the largest scales in the near wake will be on the order of the boundary layer thickness, considerably smaller than the overall scale of the wake.

Figure 7 shows the behavior of the free-surface and subsurface flow for a location one-fourth of one ship length aft of the model ($x = 1/4L$), with a model velocity of 1.48 m/s. The scale for the free-surface and subsurface images are the same. In Figure 7a the model is unpropelled (with no propeller attached), while the images in Figure 7b have the right-hand rotating propeller on the model. The location of the free

surface can be seen in the figures by the straight, vertically symmetric line of light created by the dye image and its reflection in the surface of the water. From these figures, it is clear that the turbulent fluid, marked by the dye, at the free-surface corresponds to the free-surface turbulent wake region seen in the shadowgraph images. This implies that the organized waves which lie outside the region where the subsurface wake is marked are manifestations of the free-surface disturbances in the turbulent region, generated by subsurface turbulence, but are themselves strictly free-surface phenomena.

In Figure 8, the screen is centered 0.5 m to the starboard side of the wake centerline. The model ship velocity is 1.48 m/s and the images are located at $x = 1/4L$, $1/2L$, and L. These off-center images clearly show the organized waves at the edges of the turbulent wake. The contrast between the turbulent wake and the irrotational free stream is very clear. The distance to which groups of unsteady, organized waves propagate into the irrotational free stream increases with the increase in the distance aft of the ship. Also notable at $x = L$ are the existence of these organized waves with relatively little visible free-surface disturbance in the center region of the turbulent wake.

Figures 6 and 8 show snapshots of the free-surface features visualized using the shadowgraph technique. To examine the overall free-surface features of the turbulent wake, a series of shadowgraph images such as those shown in Figure 8 were ensemble averaged. In this approach, the random free-surface fluctuations thend to cancel out and the steady, or more organized, features reinforce. Figure 9 shows averaged shadowgraph images corresponding to those in Figure 8. These images result from averaging twenty independent, uncorrelated images.

In Figure 9, the inner region of the steady, Kelvin wave pattern is clearly visible in the right-hand portion of the field of view. As in the instantaneous shadowgraph images,

there are no apparent turbulent disturbances in this outer region. Near the wake centerline, the left edge of the images, the turbulent region of the wake is clearly visible. This region, most visible in the wake of the propelled model, grows slowly in lateral extent, and the disturbances become less pronounced with distance aft. Between the region of turbulent flow and the Kelvin wave pattern there is a region of wavefronts aligned at a small angle relative to the wake centerline. This region corresponds to the organized waves identified in the instantaneous shadowgraph images. This region moves laterally more quickly than the growth of the turbulent wake and by $x = L$, this group of disturbances is distinct from the turbulent region of the wake, separated by an area of relatively calm water. Again, this behavior is most pronounced in the propelled case. The features are similar in the unpropelled case but are more difficult to distinguish due to the generally lower level of turbulent disturbances in that case.

The unsteady, small-scale, surface disturbances which appear in the turbulent wake propagate in all directions and interact with other disturbances, as well as with the unsteady surface currents, which exist in this region. After a short distance, disturbances which are moving outward, away from the turbulent region, coalesce into organized waves which propagate into the irrotational free-stream. The propagation of the outward moving disturbances through the velocity distribution of the wake may enhance the organizing process. These organized waves may be related to the observed bright "vee" signatures of surface ship wakes (see Munk *et al.* [1]). If these waves are indeed responsible for this feature of SAR images, it should be noted that this mechanism for producing short waves aligned at small angles to the ship track is independent of the Kelvin wave pattern and any large-scale coherent vortical structure, and does not require the presence of ambient waves.

Summary and conclusions

This study used a subsurface fluorescent dye visualization technique and shadowgraph visualization of free-surface disturbances to examine the evolution of the turbulent wake of a model ship and the interaction of the turbulence with the free surface. Visualization of the subsurface turbulent wake showed there was no separation of turbulent boundary layer fluid from the model ship hull resulting in the formation of bilge vortices. There is a pair of inboard rotating circulation cells that form in the cavities on either side of the rudder (stern vortices). These regions appear to be highly turbulent, with small mean circulation and, in the unpropelled case, interact to carry a portion of the turbulent wake fluid downward, away from the free surface. Near the free surface a thin (relative to the width of the wake) region of turbulent fluid grows laterally outward beneath, and adjacent to, the free surface resulting in a characteristic "tee" shape for the wake. These results, when combined with those of Anthony [10] show that turbulence near the free surface is sufficient to generate a diverging surface current, and that large-scale coherent vortices are not required.

The addition of a right-hand rotating propeller results in an increased rate of growth for the wake. This is probably due to higher turbulence levels resulting from the increased momentum in the wake. Also, the rotating propeller tends to confine the subsurface wake and reduce the downward movement, but does not alter the overall shape of the subsurface wake. This suggests that the development of the wake is primarily hull dependent, at least for single-screw ships

The free surface in the turbulent wake, when visualized using the shadowgraph technique, exhibits irregular surface disturbances for distances less than about two ship-lengths aft. This region corresponds directly with the thin turbulent surface layer identified

in the subsurface visualization. At the edges of the turbulent region, small-scale, unsteady waves appear which propagate outward. After a short distance, these small-scale disturbances coalesce into somewhat organized waves which propagate into the irrotational free-stream. This behavior was confirmed by ensemble-averaged shadowgraph images which showed them to be a consistent feature, distinct from the random free-surface disturbances in the turbulent region of the wake, and also distinct from the steady Kelvin wave pattern. These organized waves may be related to the observed radar signatures of surface ship wakes, and show that short, organized waves propagating at small angles relative to the ship track can be generated by turbulent surface disturbances. This mechanism is independent of the Kelvin wave pattern and does not rely on the presence of ambient waves or large-scale coherent vortices.

The addition of the right-hand rotating propeller decreased the turbulent surface activity near the center of the wake but increased the activity near the edges of the wake, particularly on the starboard side. The organized waves on the outer edges of the wake show a significant increase in amplitude as well. The increase in overall surface activity confirms an increase in turbulent activity in the subsurface turbulent wake region due to the propeller.

This work was funded by the Office of Naval Research under the University Research Initiative Program in Ship Hydrodynamics contract number N000184-86K-0684. This support is gratefully acknowledged. The authors also wish to thank A. Reed and W. Lindenmuth of the David Taylor Research Center for making the *Quapaw* model available.

References

1 Munk, W.H., Scully-Power, P., & Zachariasen, F., "Ship wakes from space: The Bakerian Lecture, 1986," Proc. Royal Soc. London A, Vol. 412, 1987, pp. 231-254.

2 Lyden, J.D., Hammond, R.R., Lyzenga, D.R. & Schuchman, R.A., "Synthetic aperture radar imaging of surface ship wakes," J. Geophys. Rsch, Vol. 93, C10, 1988.

3 Peltzer, R.D., Griffin, O.M., Kaiser, J.C., & Barger, W.R., "Redistribution of surface-active materials in a ship wake," Dynamics of Bubbles and Vortices Near a Free Surface–AMD 119, ASME, 1991, pp. 89-103.

4 Milgram, J.H., "Theory of radar backscatter from short waves generated by ships with application to radar (SAR) imagery," J. Ship Research, Vol. 32, 1988, p. 54.

5 Hughes, B.A., Surface wave wakes and internal wave wakes produced by surface ships, Defense Research Establishment Pacific, Forces Mail Office, Victoria, B.C. VOS 1B0, 1986.

6 Griffin, O.M., "Ship wave modification by a surface current field," J. Ship Research, Vol. 32, 1988, p. 186.

7 Lugt, H.J., Vortex Flow in Nature and Technology, Wiley-Interscience, New York, 1983.

8 Ramberg, S.E., Swean, T.F. & M.W. Plesnia., "Turbulence near a free surface in a plane jet," NRL Memorandum Report 6367, Naval Research Laboratory, Washington, D.C., 1989

9 Madnia, K., Interaction of a turbulent round jet with the free surface, Ph.D. Dissertation, The University of Michigan, Ann Arbor Michigan, 1988.

10 Anthony, D.G., Willmarth, W.W., Madnia, K. & Bernal, L.P., "Turbulence measurements in a submerged jet near a free surface," Preprints 18th Symposium on Naval Hydrodynamics. University of Michigan, Ann Arbor, Michigan, 1990.

11 Bernal, L.P. & Madnia, K., "Interaction of a turbulent round jet with the free surface," Proc. 17th Symp. on Naval Hydro., The Hague, Netherlands, 1988.

12 Sterling, M.H., Gorman, M., Widmann, P.J., Coffman, S.C., Strozier,J. & Kiehn, R.M., "Why are these disks dark? The optics of Rankine vortices," Phys. Fluids, Vol. 30, 1987, pp. 3624-3626.

13 Anthony, D.G., The influence of a free surface on the development of turbulence in a submerged jet, Ph.D. Dissertation, The University of Michigan, Ann Arbor Michigan, 1990.

Figure Captions

Figure 1. Model No. 3531: 1/12 scale *ATF Quapaw* body plan.

Figure 2. Experimental arrangement for fluorescent dye visualization of boundary layer and subsurface wake showing laser sheet and model basin cross section.

Figure 3. Schematic of experimental arrangement for shadowgraph imaging of free-surface features.

Figure 4. Fluorescent dye visualization of boundary layer and initial formation of subsurface wake; laser sheet located at a) $x = -1/2L$, b) $-1/4L$, c) $1/8L$, d) $1/4L$.

Figure 5. Fluorescent dye visualization of boundary layer and initial formation of subsurface wake; laser sheet located at a) $x = -1/4L$ (w/o prop), b) $x = -1/4L$ (w/prop), c) $x = -1/16L$ (w/o prop), d) $x = -1/16L$ (w/prop), e) $x = 0$ (w/o prop), f) $x = 0$ (w/prop), g) $x = 1/16L$ (w/o prop), h) $x = 1/16L$ (w/prop), i) $x = 1/4L$ (w/o prop), j) $x = 1/4L$ (w/prop), k) $x = 1L$ (w/o prop), l) $x = 1L$ (w/prop).

Figure 6. Shadowgraph images of the free-surface wake with the screen centered relative to the wake at a) $x = 1/4L$ (w/o prop), b) $x = 1/4L$ (w/prop), c) $x = 1/2L$ (w/o prop), d) $x = 1/2L$ (w/prop), e) $x = L$ (w/o prop), f) $x = L$ (w/prop), g) $x = 2L$ (w/o prop), h) $x = 2L$ (w/prop).

Figure 7. Comparison of free-surface and subsurface turbulent model ship wake at $x = 1/4L$; a) free-surface shadowgraph (w/o prop), b) free-surface shadowgraph (w/prop), c) subsurface wake (w/o prop), d) subsurface wake (w/prop).

Figure 8. Shadowgraph images of the free-surface wake with the screen 0.5 m left of the wake centerline; a) $x = 1/4L$ (w/o prop), b) $x = 1/4L$ (w/prop), c) $x = 1/2L$ (w/o prop), d) $x = 1/2L$ (w/prop), e) $x = 1$ (w/o prop), f) $x = 1$ (w/prop).

Figure 9. Twenty-frame average of shadowgraph images of the free-surface wake with the screen 0.5 m left of the wake centerline; a) $x = 1/4L$ (w/o prop), b) $x = 1/4L$ (w/prop), c) $x = 1/2L$ (w/o prop), d) $x = 1/2L$ (w/prop), e) $x = 1$ (w/o prop), f) $x = 1$ (w/prop).

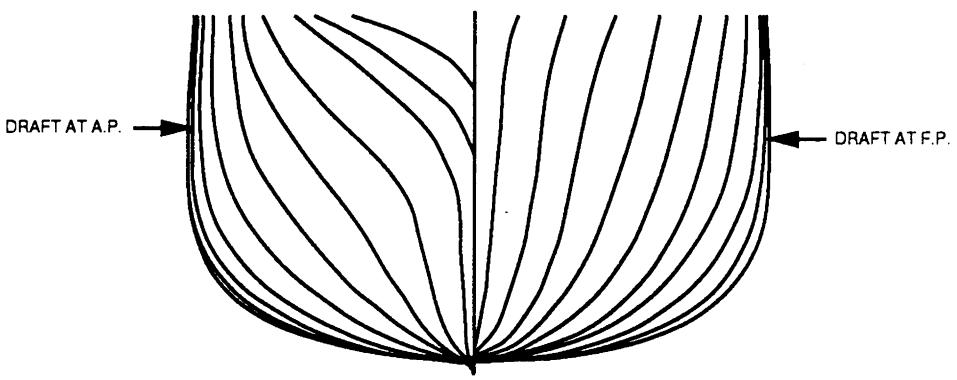

MODEL NO. 3531: 1/12 SCALE U.S.S. QUAPAW

LENGTH BETWEEN PERPENDICULARS	4.95 M
BEAM	0.98 M
DRAFT AT AFT PERPENDICULAR	0.43 M
DRAFT AT FORWARD PERPENDICULAR	0.35 M

Figure 1. Model No. 3531: 1/12 scale ATF Quapaw body plan.

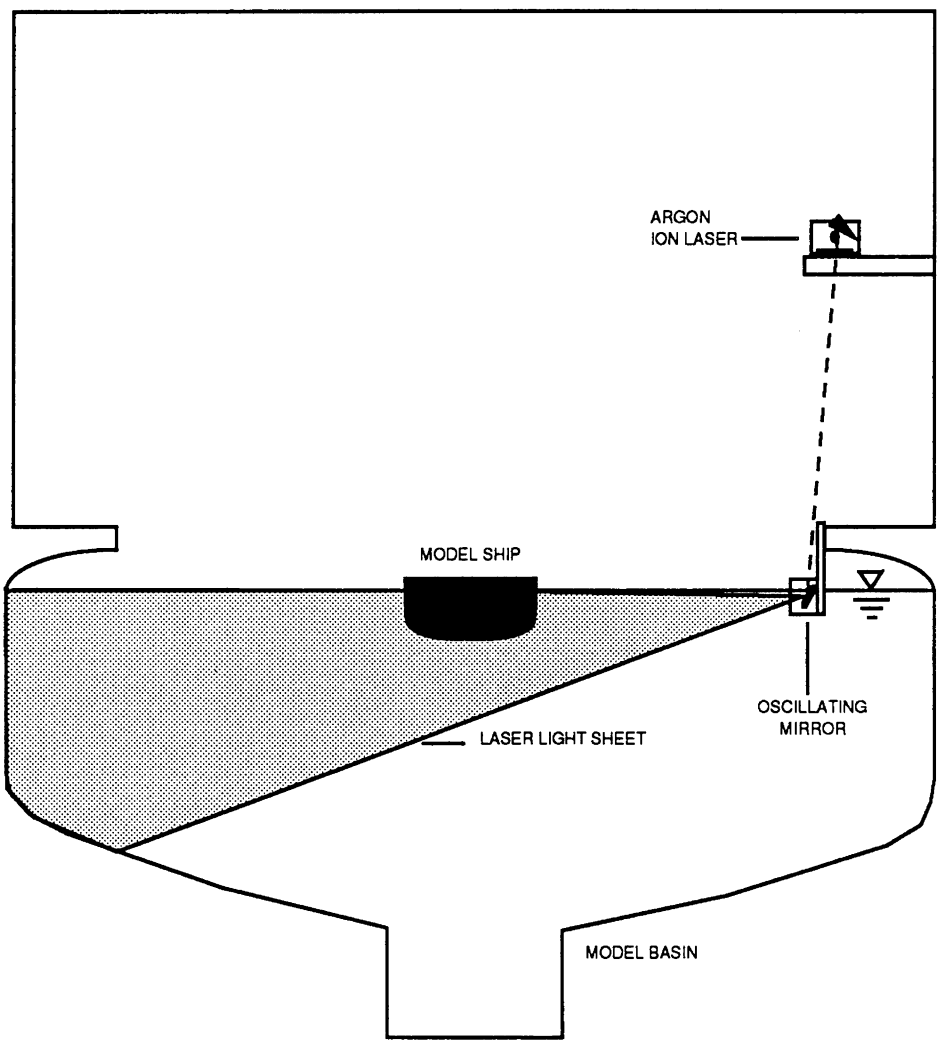

Figure 2. Experimental arrangement for fluorescent dye visualization of subsurface wake showing laser sheet and model basin cross section.

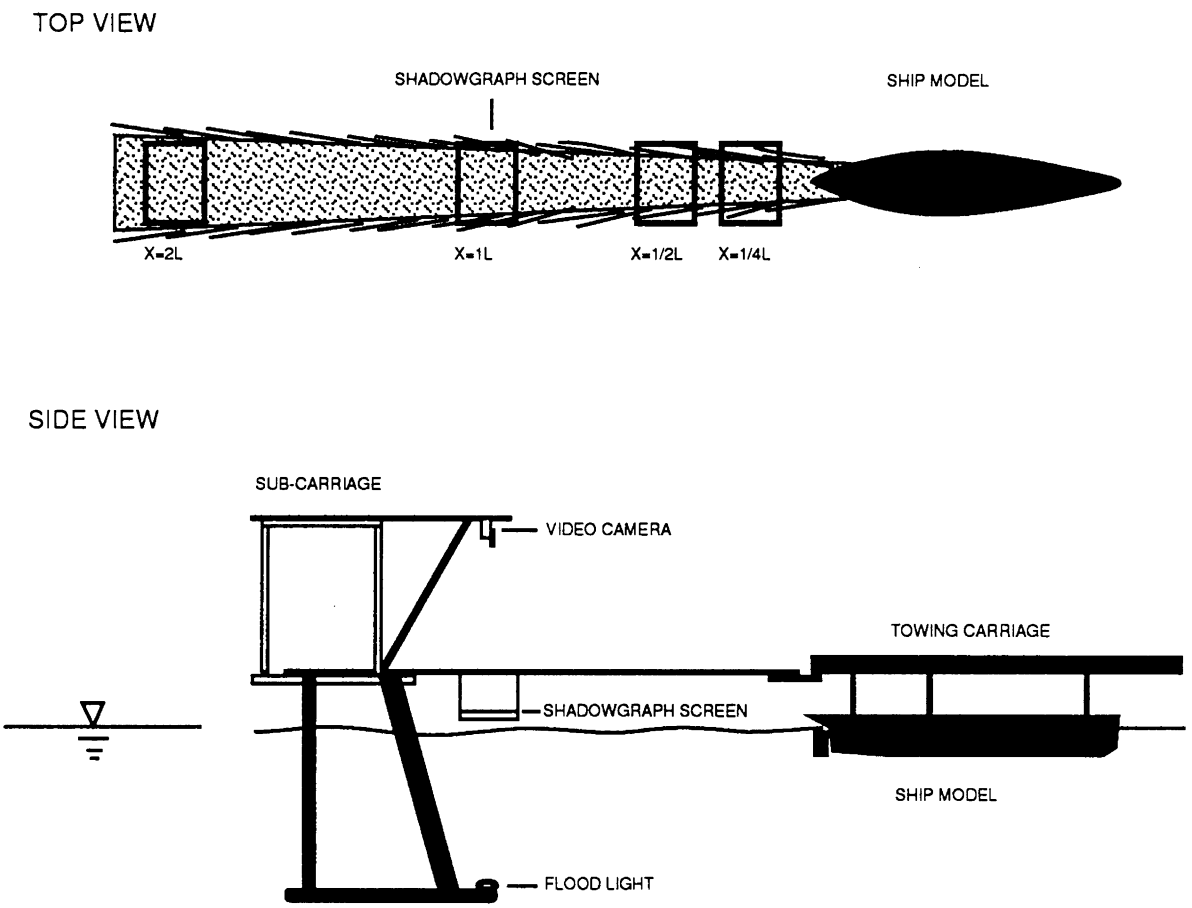

Figure 3. Schematic of the experimental arrangement used for obtaining shadowgraph images.

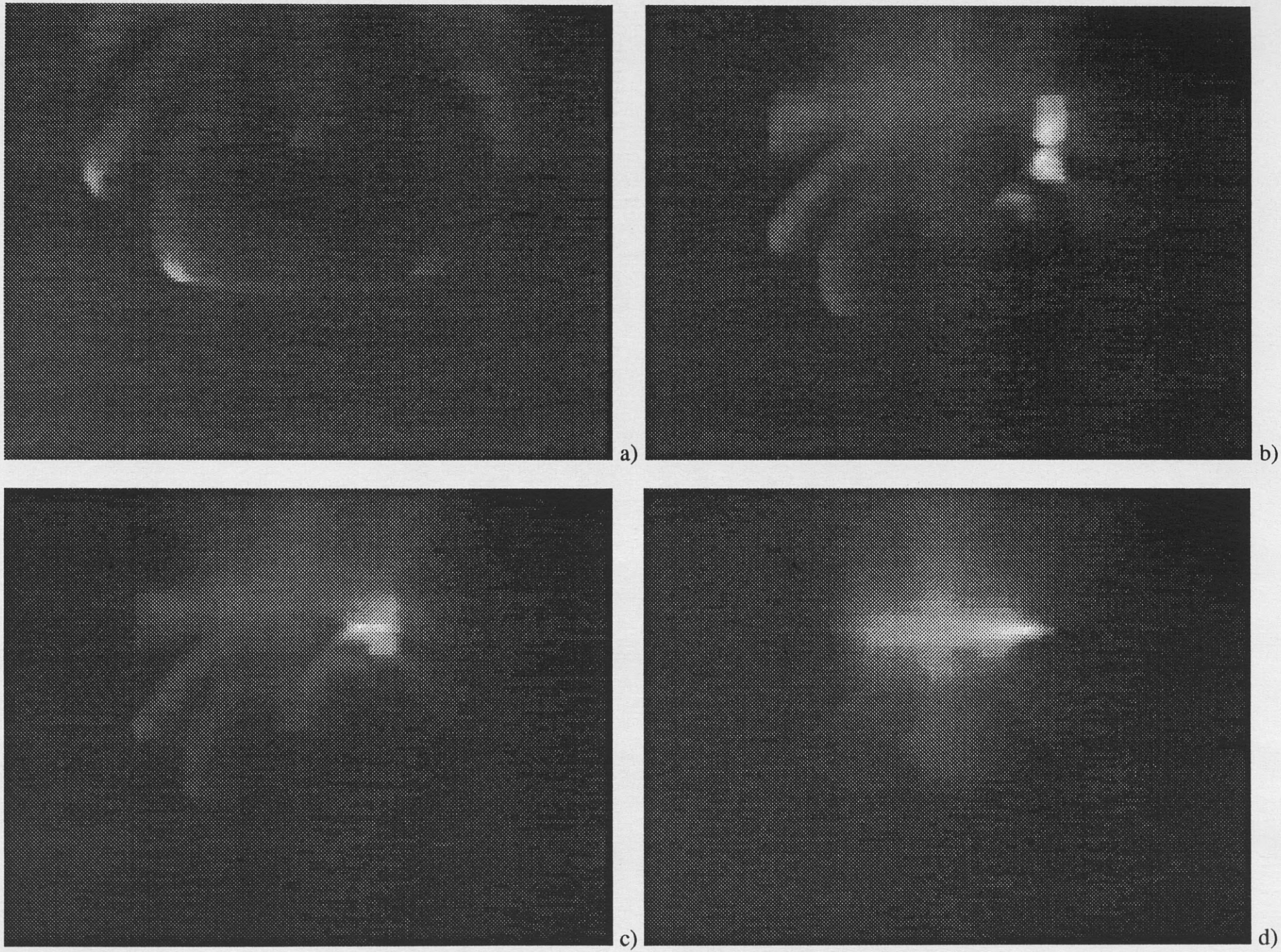

Figure 4. Fluorescent dye visualization of boundary layer and initial formation of subsurface wake; laser sheet located at a) $x = -1/2L$, b) $-1/4L$, c) $-1/8L$, d) $1/2L$.

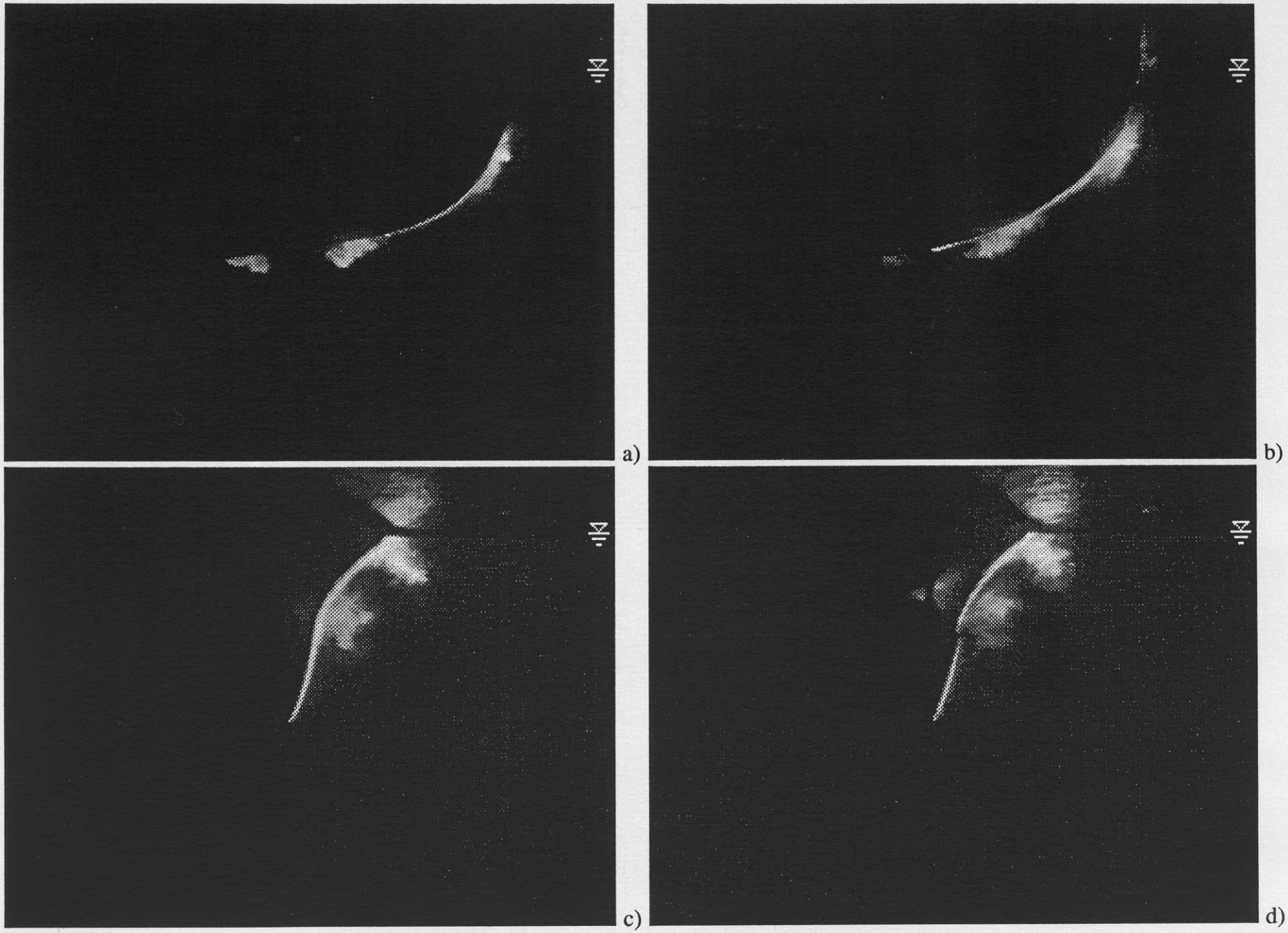

Figure 5. (continued)

e)

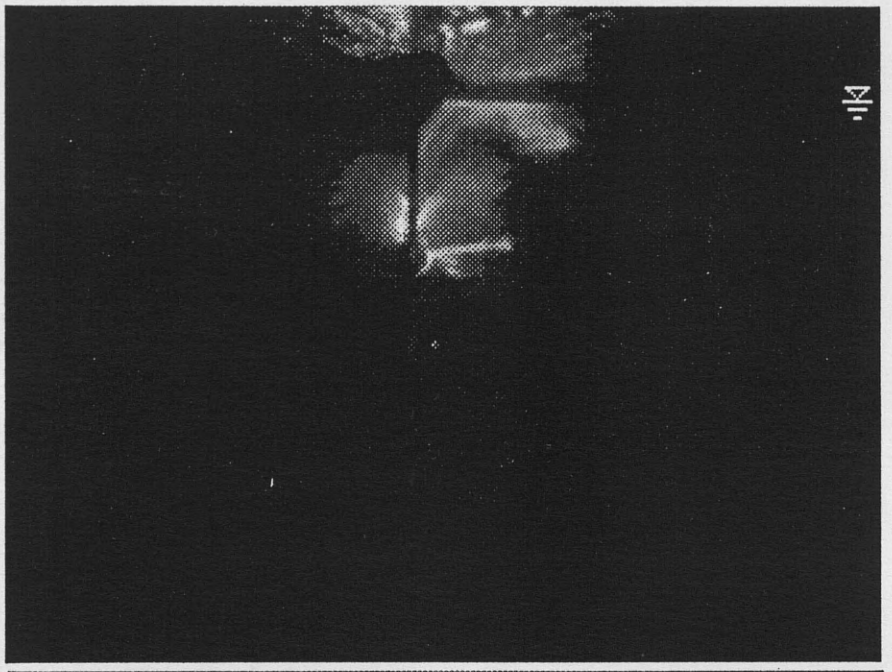

f)

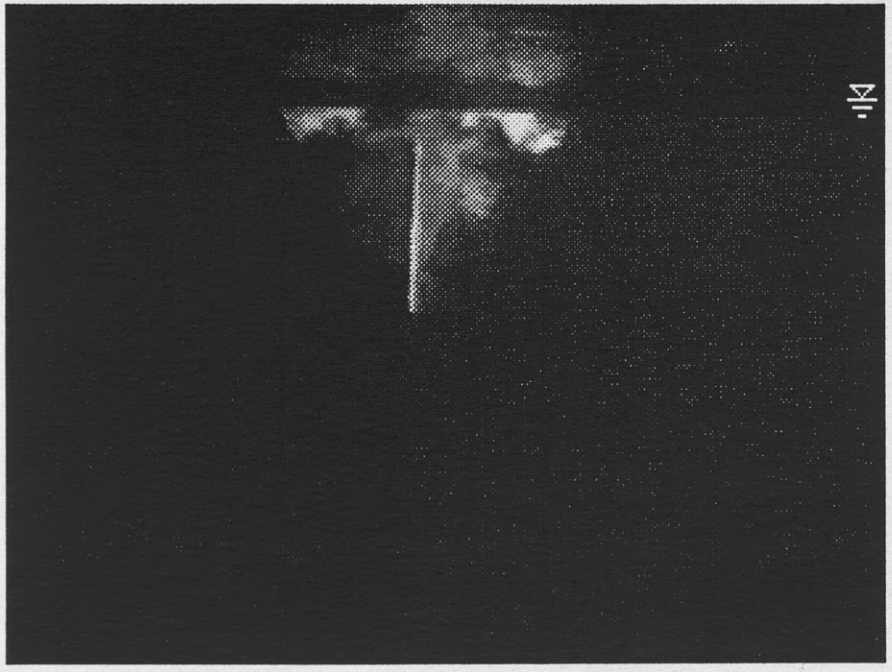

g)

h)

Figure 5. (continued)

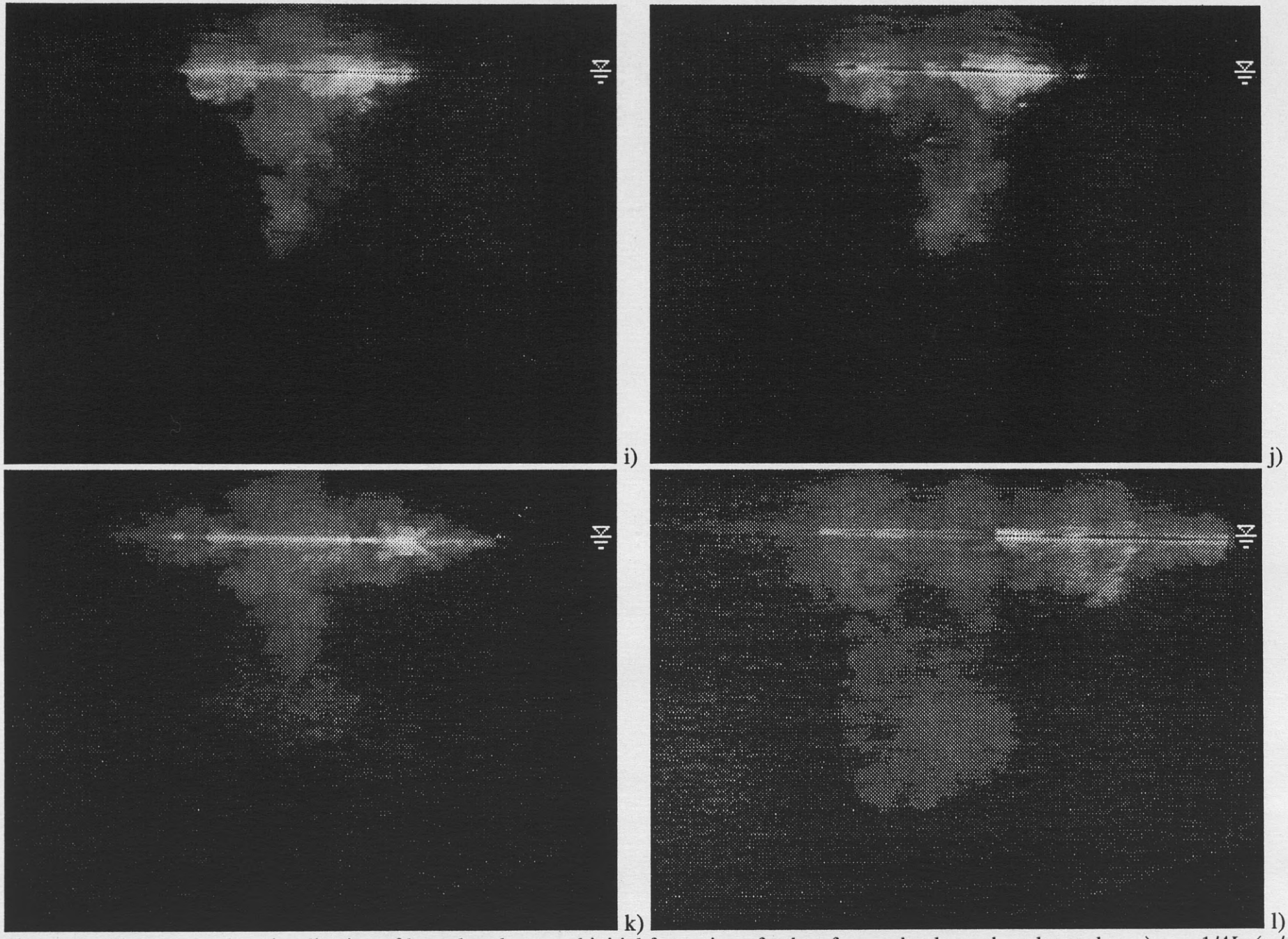

Figure 5. Fluorescent dye visualization of boundary layer and initial formation of subsurface wake; laser sheet located at a) $x = -1/4L$ (w/o prop), b) $x = -1/4L$ (w/prop), c) $x = -1/16L$ (w/o prop), d) $x = -1/16L$ (w/prop), e) $x = 0$ (w/o prop), f) $x = 0$ (w/prop), g) $x = 1/16L$ (w/o prop), h) $x = 1/16L$ (w/prop), i) $x = 1/4L$ (w/o prop), j) $x = 1/4L$ (w/prop), k) $x = 1L$ (w/o prop), l) $x = 1L$ (w/prop).

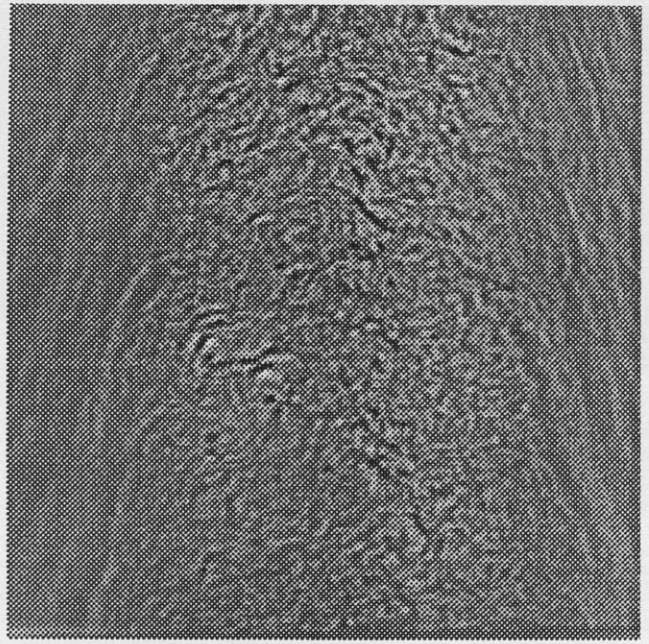

a)

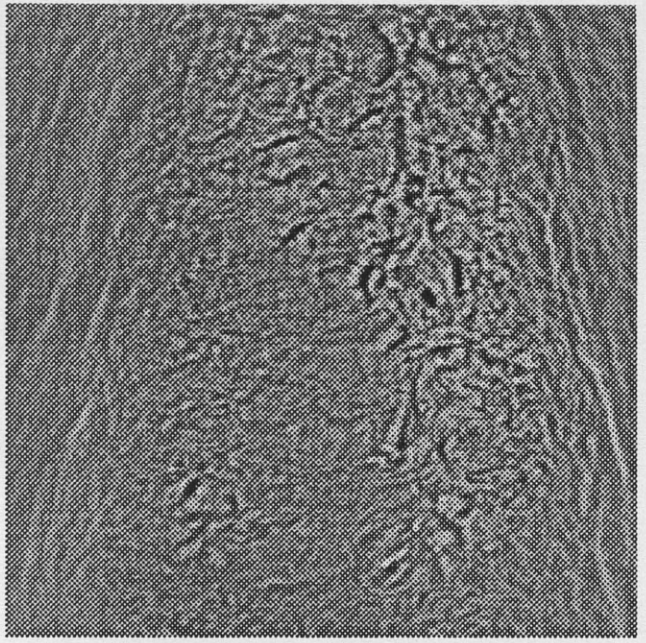

b)

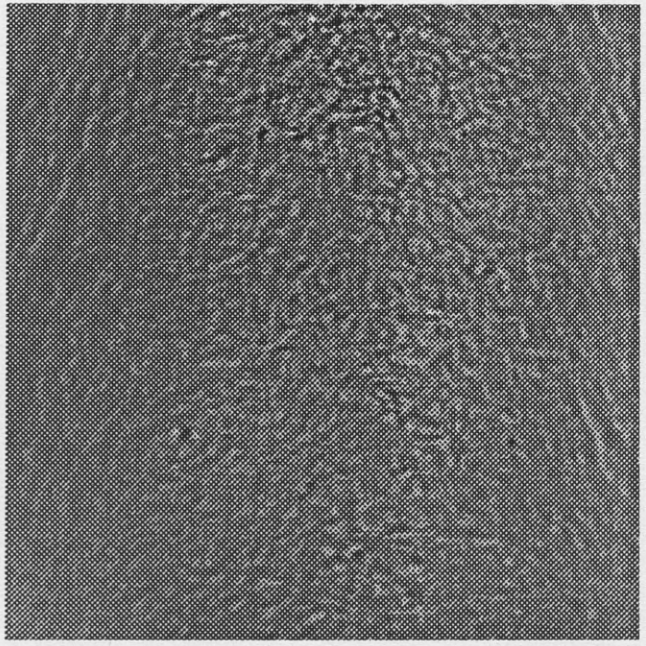

c)

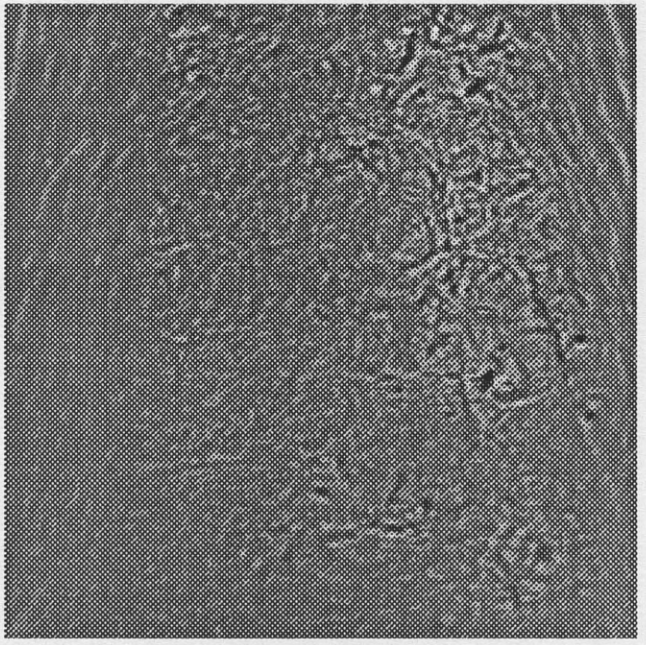

d)

Figure 6. (continued)

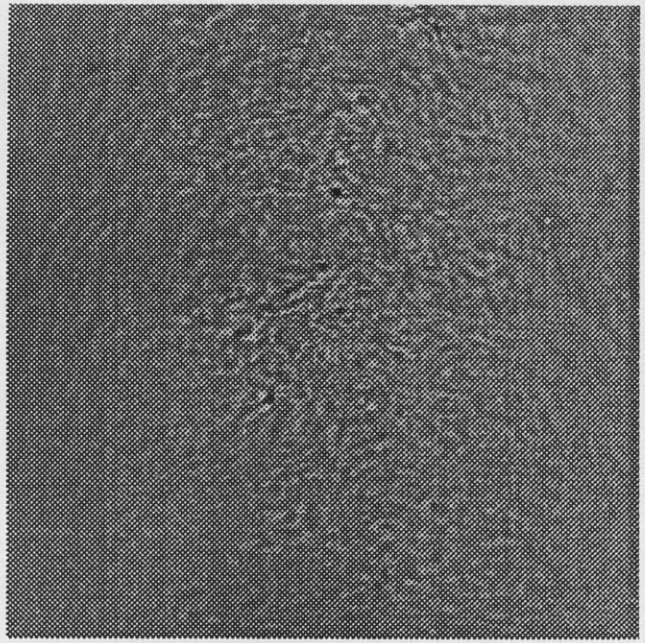

e)

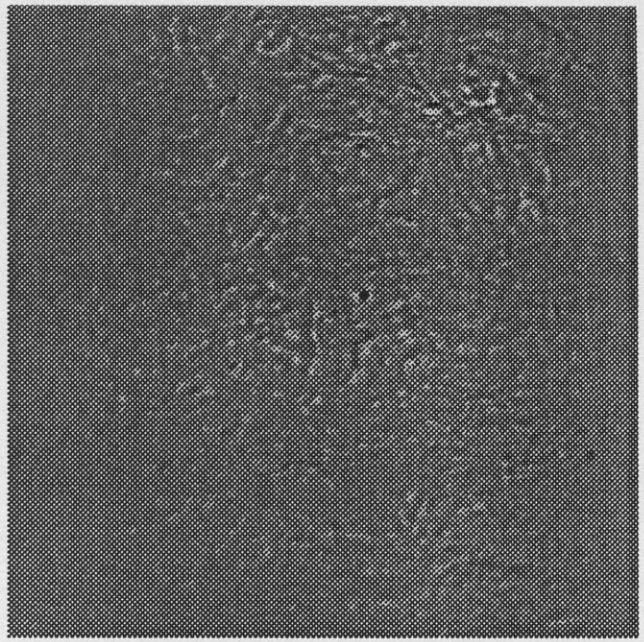

f)

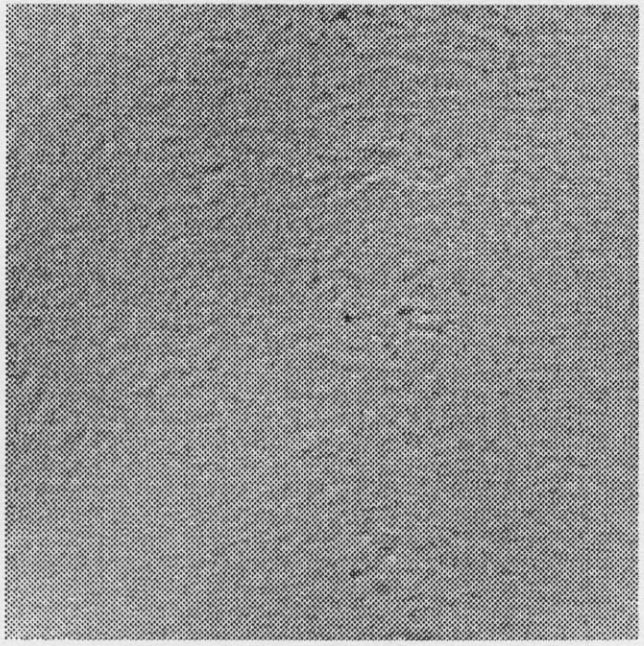

g)

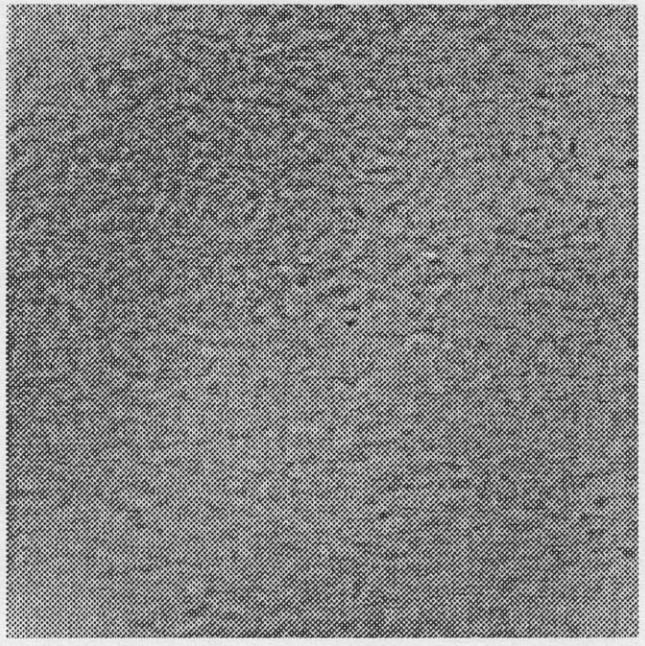

h

Figure 6. Shadowgraph images of the free-surface wake with the screen centered relative to the wake at a) $x = 1/4L$ (w/o prop), b) $x = 1/4L$ (w/prop), c) $x = 1/2L$ (w/o prop), d) $x = 1/2L$ (w/prop), e) $x = L$ (w/o prop), f) $x = L$ (w/prop), g) $x = 2L$ (w/o prop), h) $x = 2L$ (w/prop).

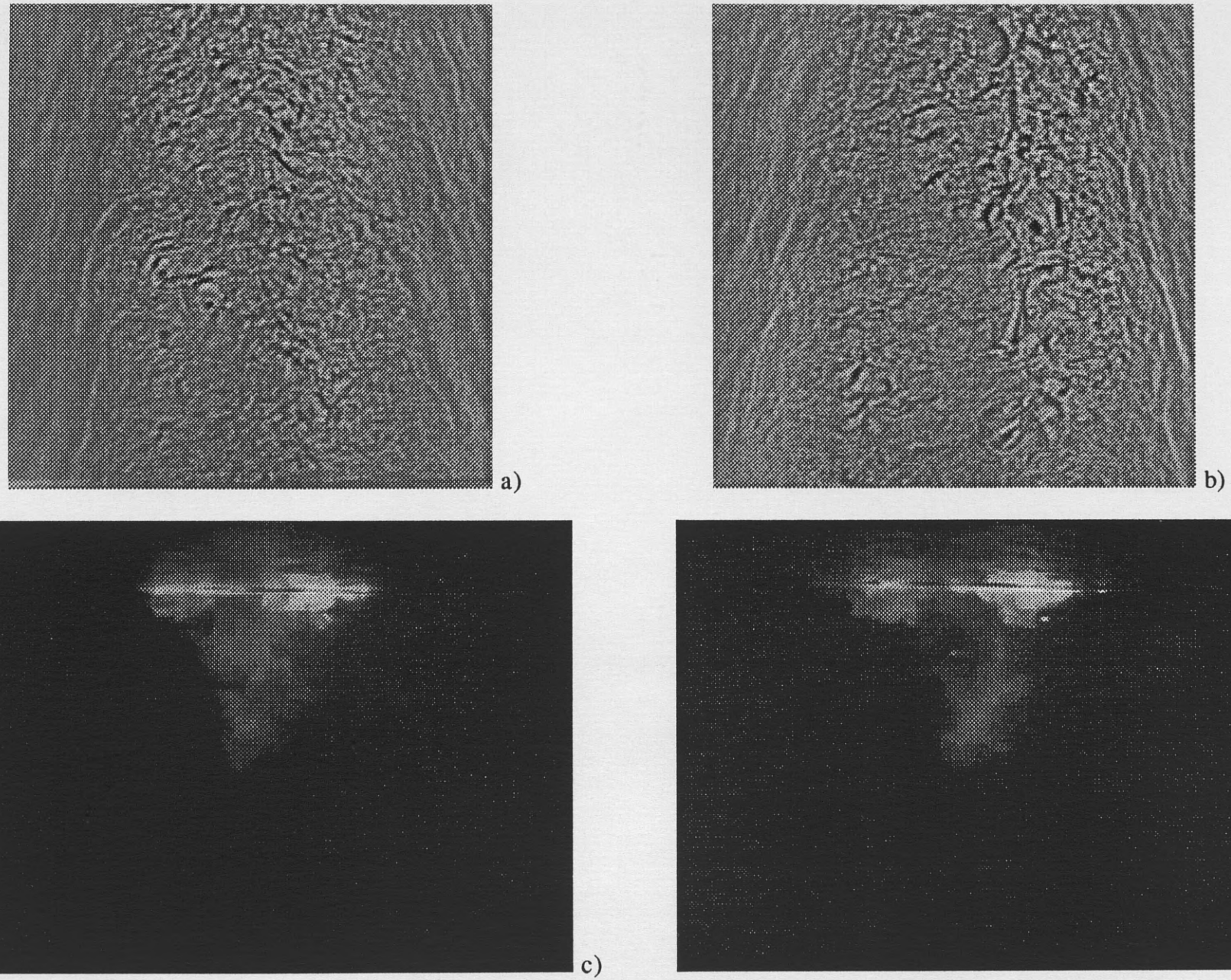

Figure 7. Comparison of free-surface and subsurface turbulent model ship wake at $x = 1/4L$; a) free-surface shadowgraph (w/o prop), b) free-surface shadowgraph (w/prop), c) subsurface wake (w/o prop), d) subsurface wake (w/prop).

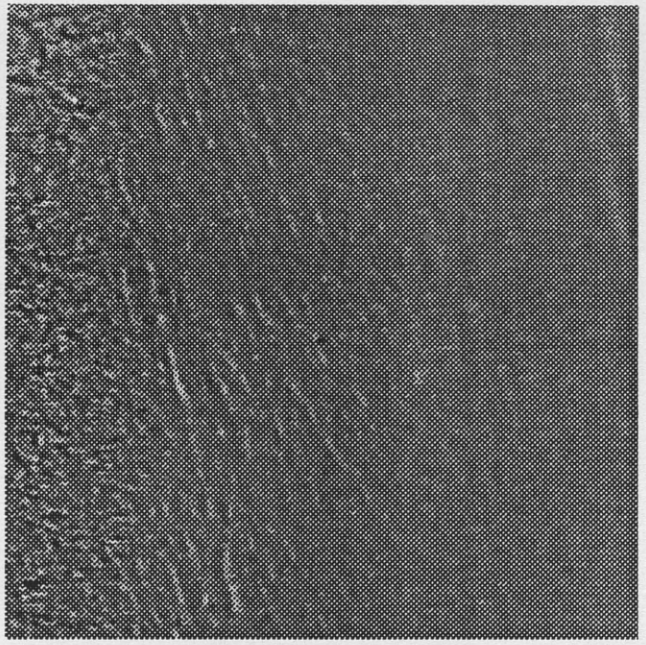

a)

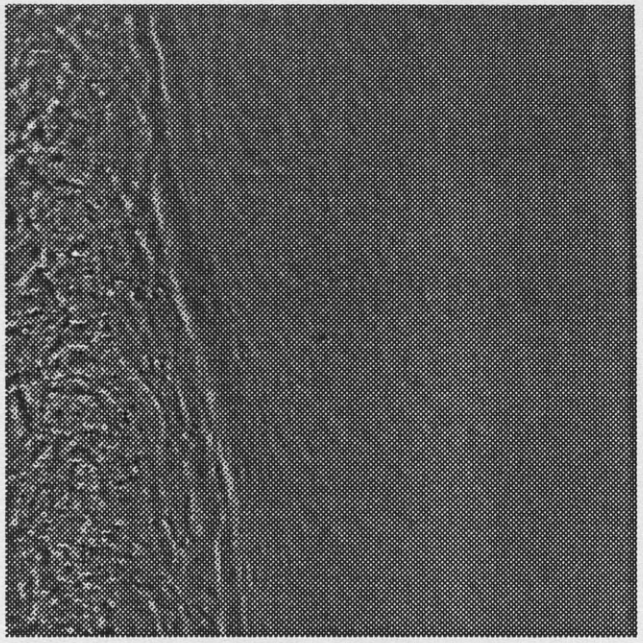

b)

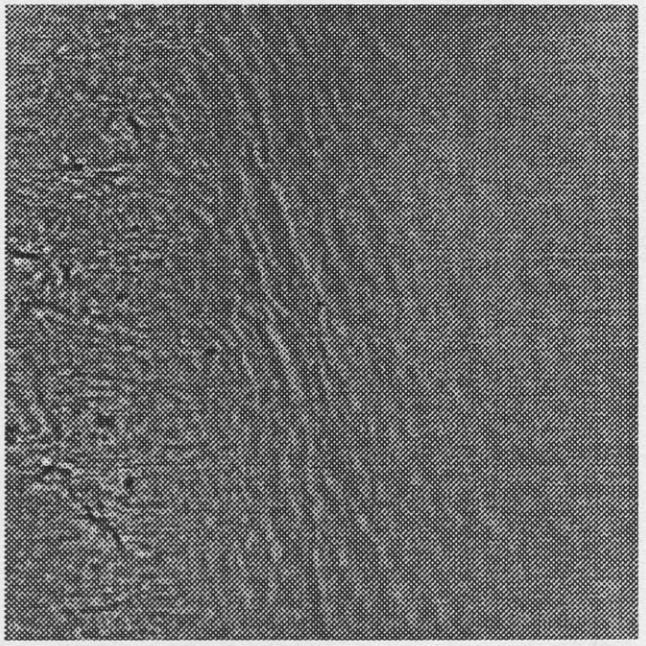

c)

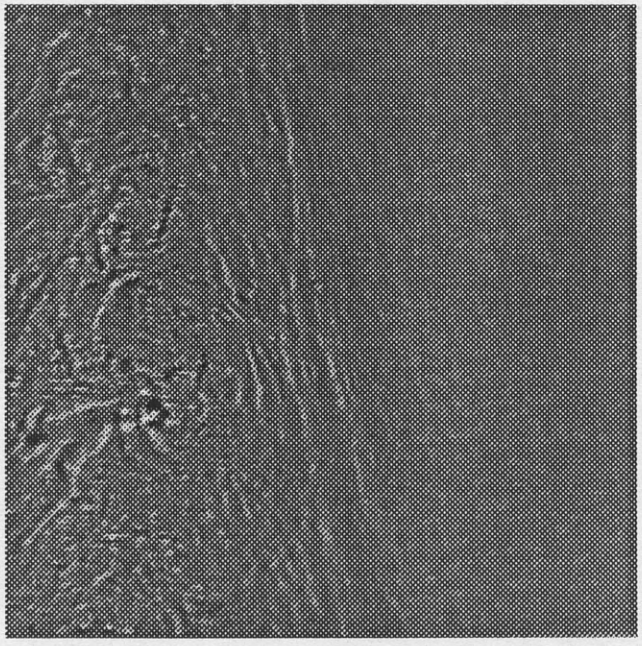

d)

Figure 8. (continued)

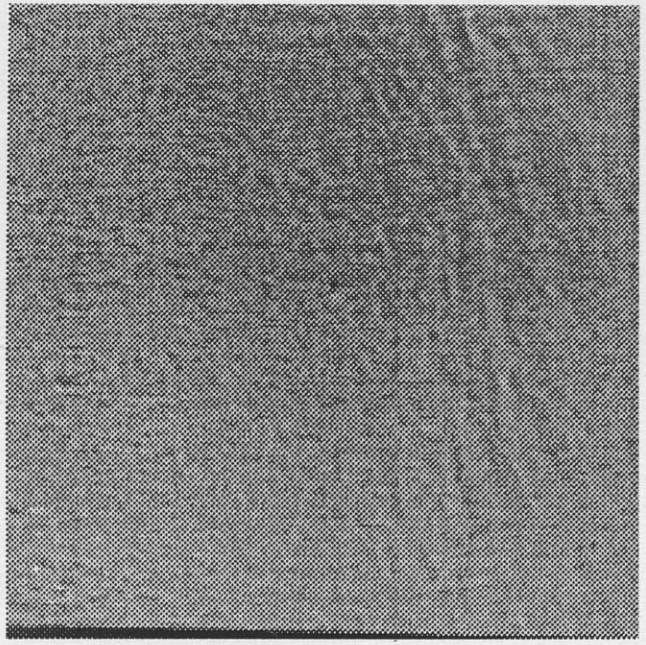

e)

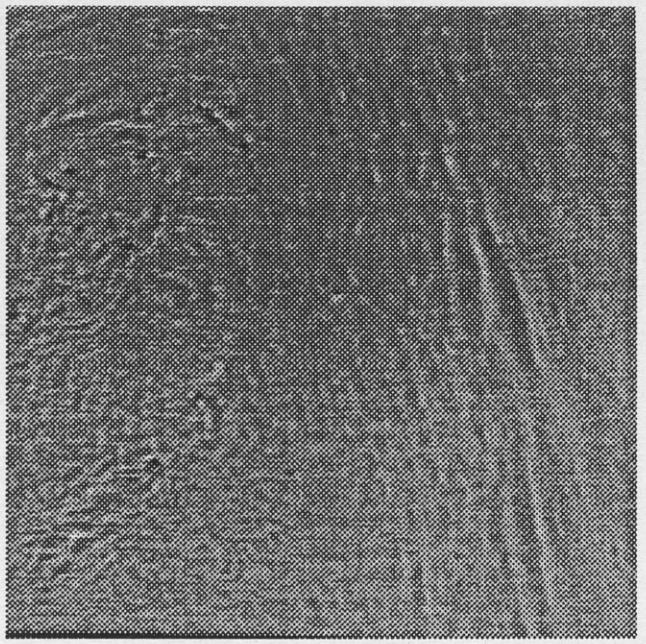

f)

Figure 8. Shadowgraph images of the free-surface wake with the screen 0.5 m left of the wake centerline; a) $x = 1/4L$ (w/o prop), b) $x = 1/4L$ (w/prop), c) $x = 1/2L$ (w/o prop), d) $x = 1/2L$ (w/prop), e) $x = 1$ (w/o prop), f) $x = 1$ (w/prop).

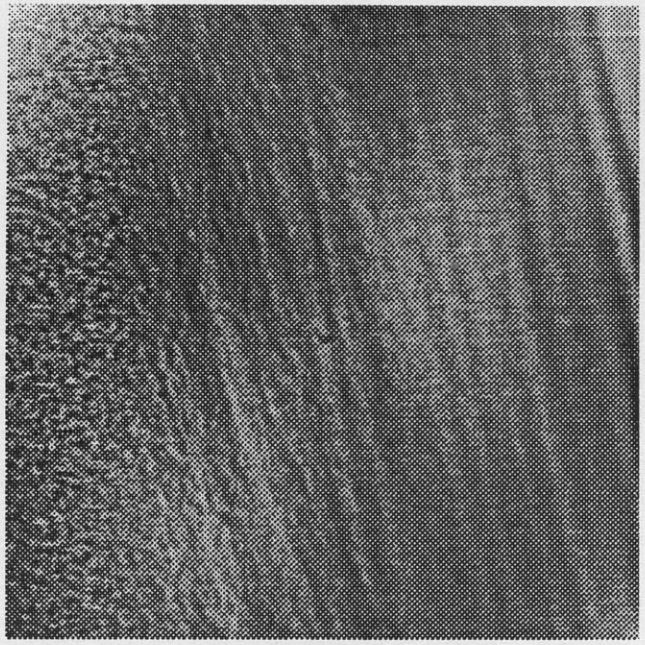

a)

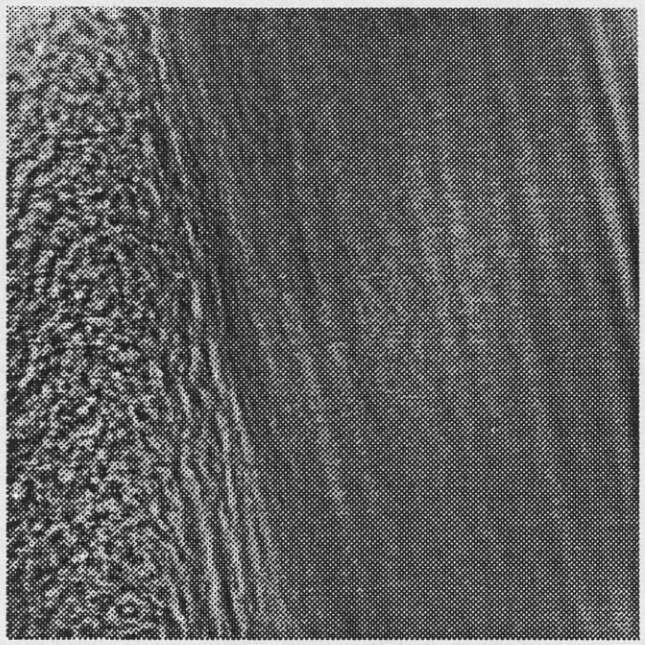

b)

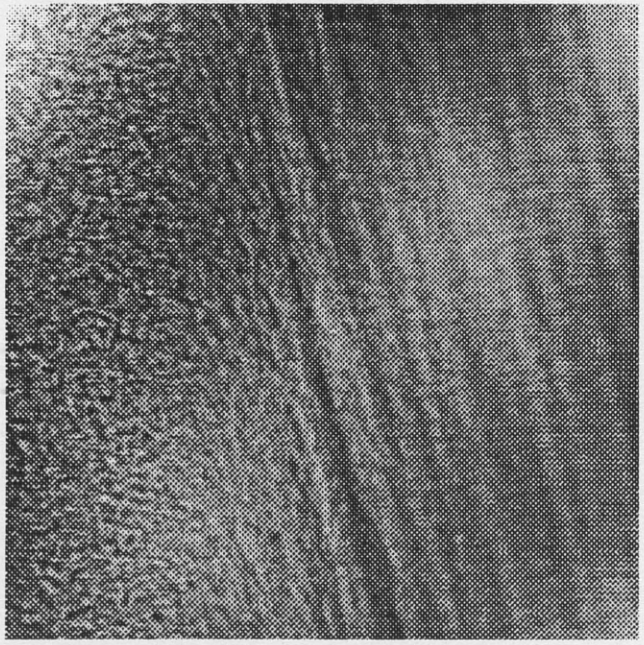

c)

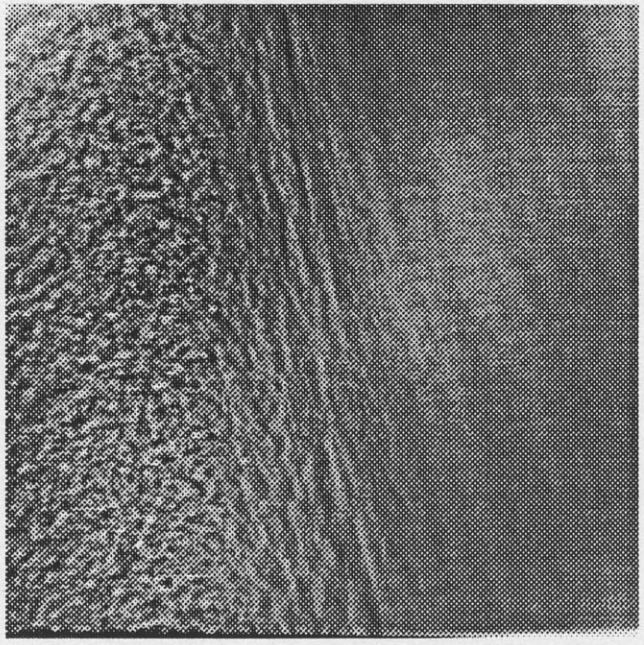

d)

Figure 9. (continued)

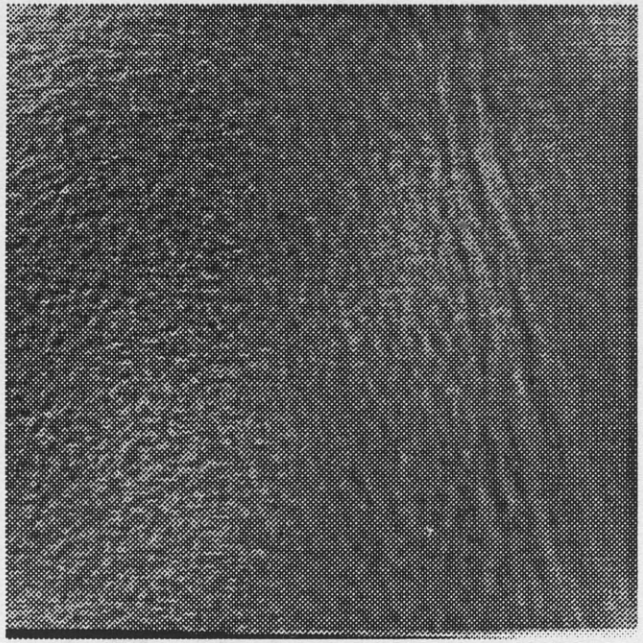

e)

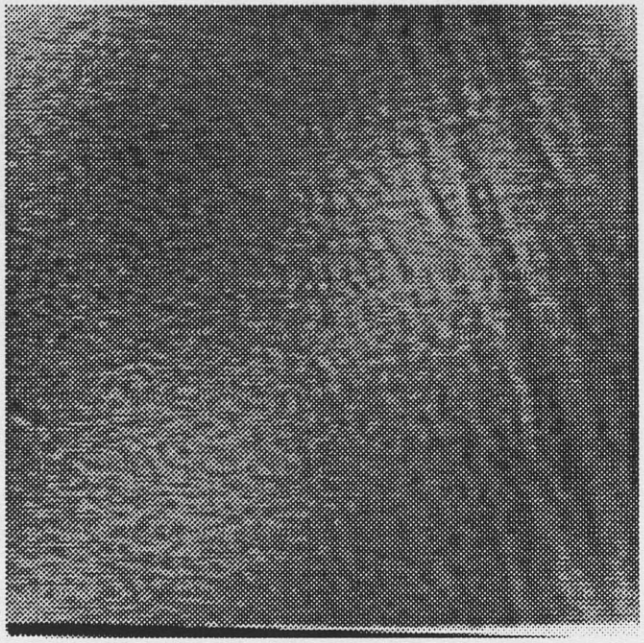

f)

Figure 9. Twenty-frame average of shadowgraph images of the free-surface wake with the screen 0.5 m left of the wake centerline; a) $x = 1/4L$ (w/o prop), b) $x = 1/4L$ (w/prop), c) $x = 1/2L$ (w/o prop), d) $x = 1/2L$ (w/prop), e) $x = 1$ (w/o prop), f) $x = 1$ (w/prop).